THE ROYAL SOCIETY

Published online 22 August 2003

Finite element modelling of contracting skeletal muscle

C. W. J. Oomens[1*], M. Maenhout[1], C. H. van Oijen[1], M. R. Drost[2] and F. P. Baaijens[1]

[1]*Department of Biomedical Engineering, Eindhoven University of Technology, PO Box 513, 5600 MB Eindhoven, The Netherlands*

[2]*Department of Movement Sciences, University of Maastricht, PO Box 616, 6200 MD Maastricht, The Netherlands*

To describe the mechanical behaviour of biological tissues and transport processes in biological tissues, conservation laws such as conservation of mass, momentum and energy play a central role. Mathematically these are cast into the form of partial differential equations. Because of nonlinear material behaviour, inhomogeneous properties and usually a complex geometry, it is impossible to find closed-form analytical solutions for these sets of equations. The objective of the finite element method is to find approximate solutions for these problems.

The concepts of the finite element method are explained on a finite element continuum model of skeletal muscle. In this case, the momentum equations have to be solved with an extra constraint, because the material behaves as nearly incompressible. The material behaviour consists of a highly nonlinear passive part and an active part. The latter is described with a two-state Huxley model. This means that an extra nonlinear partial differential equation has to be solved. The problems and solutions involved with this procedure are explained. The model is used to describe the mechanical behaviour of a tibialis anterior of a rat. The results have been compared with experimentally determined strains at the surface of the muscle. Qualitatively there is good agreement between measured and calculated strains, but the measured strains were higher.

Keywords: finite element model; skeletal muscle; Huxley equation; distributed moments

1. INTRODUCTION

To describe the mechanical behaviour of biological structures, conservation laws such as the balance of mass, momentum and energy play a central role. These balance laws, together with constitutive equations, describing the material properties, and boundary and initial conditions make it possible to mathematically solve a large variety of problems, related to the functioning of biological systems. The balance laws and constitutive equations form a set of partial differential equations.

Many 'soft' biological materials undergo large deformations (strains up to 100%) and large rigid-body motions, meaning that a geometrically nonlinear theory has to be used. Moreover, the constitutive equation, i.e. the relationship between stress and applied strain in the material, is usually nonlinear, anisotropic and inhomogeneous. Finally, the geometry of the object being studied is complex. Consequently, closed-form solutions of the mathematical equations cannot be found for non-trivial problems. A powerful tool to find good approximate numerical solutions for these equations is the finite element method. This method transforms the partial differential equations into a finite set of algebraic equations. This is accomplished by using an equivalent integral expression of the partial differential equations (e.g. via the use of weighted residuals formulation) and appropriate spatial and temporal discretization.

The objective of the present paper is to explain the concepts of a finite element model of contracting skeletal muscle. Because the paper was part of a symposium on 'modelling in biomechanics', it is more focused on the concept than on the results. A model for contracting skeletal muscle is chosen to elaborate on the solution strategy and on some of the specific problems, typical for contracting muscle. To stay within the scope of the journal, the mathematics is kept to a minimum. For a more extensive treatment of the subject, the reader is referred to an excellent textbook on the finite element method (Zienkiewicz & Taylor 1989) and some recent publications on skeletal muscle models (Gielen *et al.* 2000; Maenhout 2002). In § 2 the physics of the model and the governing equations will be summarized. After that, the solution process is described in more detail. The paper ends with an example of a simulation and some concluding remarks.

2. MODEL DESCRIPTION

The objective was the development of a continuum model for contracting skeletal muscle that may be used as a tool for studies on damage and adaptation of this tissue.

* Author for correspondence (c.w.j.oomens@tue.nl).

One contribution of 20 to a Theme Issue 'Modelling in biomechanics'.

A continuum model was necessary, because the work is based on the hypothesis that local stresses and strains result in local changes of the muscle tissue.

The basics of such a model are the balance of momentum and the balance of mass (Hunter 1983). The model was meant as a tool in research on the development of pressure sores and to study Pompe's disease. This means that very fast movements of the muscle do not occur and thus inertial forces and body forces can be ignored. In that case the momentum balance reduces to a set of equilibrium equations for the stresses:

$$\nabla\cdot\boldsymbol{\sigma} = 0. \tag{2.1}$$

In equation (2.1) $\boldsymbol{\sigma}$ is called the Cauchy stress tensor, and ∇ is the gradient operator with respect to the current configuration. Equation (2.1) represents a set of partial differential equations with derivatives to each of the coordinate directions. Because we are dealing with a continuum, the equation has to be applied at each point in space.

The deformation tensor $\boldsymbol{F}$ is a mapping of the undeformed reference configuration on the deformed configuration. Consider an infinitesimal line element $d\boldsymbol{x}_0$ in the undeformed reference configuration. After deformation this line element is rotated and deformed to line element $d\boldsymbol{x}$. $\boldsymbol{F}$ is a mapping of the undeformed reference configuration on the deformed configuration:

$$d\boldsymbol{x} = \boldsymbol{F}\cdot d\boldsymbol{x}_0. \tag{2.2}$$

Muscle consists of more than 70% water and behaves as nearly incompressible. Nearly and fully incompressible material behaviour can lead to 'locking' of elements in a numerical procedure. This becomes visible as oscillations in the displacement fields. For this reason it is better to consider the material fully incompressible and account for it properly in the numerical procedure.

Incompressibility is taken into account by an extra constraint that the determinant of $\boldsymbol{F}$ equals 1:

$$\det\boldsymbol{F} = 1. \tag{2.3}$$

The determinant $\det\boldsymbol{F}$ is a measure of the volume change.

The above equations are general equations, not specific for any type of material. Beside these equations, we need constitutive equations, specific for the material under consideration, relating the stress $\boldsymbol{\sigma}$ to the applied strain F. There are numerous ways to do this. The correct equation can be determined only by means of experiments.

For skeletal muscle, the following choice was made. It is assumed that the total stress in the material is defined by a superposition of a passive stress (caused by the stiffness properties of collagen and cytoskeletal materials) and an active stress that works only in the fibre direction (Gielen *et al.* 2000). In mathematical terms this can be written as

$$\boldsymbol{\sigma} = \boldsymbol{\sigma}_{\text{passive}} + \boldsymbol{\sigma}_{\text{active}}\boldsymbol{e}_{\text{f}}\boldsymbol{e}_{\text{f}}, \tag{2.4}$$

where $\boldsymbol{e}_{\text{f}}$ denotes the local fibre direction. The following nonlinear relationship between stress and strain is chosen for the passive stress:

$$\boldsymbol{\sigma} = \boldsymbol{\sigma}_{\text{matrix}} + \boldsymbol{\sigma}_{\text{fibre}}\boldsymbol{e}_{\text{f}}\boldsymbol{e}_{\text{f}}, \tag{2.5a}$$

$$\boldsymbol{\sigma}_{\text{matrix}} = G(\boldsymbol{F}\cdot\boldsymbol{F}^{\text{T}} - \boldsymbol{I}) - p\boldsymbol{I}, \tag{2.5b}$$

$$\boldsymbol{\sigma}_{\text{fibre}} = m_1\lambda^2(\mathrm{e}^{m_2(\lambda^2-1)} - 1) \quad \text{if } \lambda \geqslant 1,$$
$$\boldsymbol{\sigma}_{\text{fibre}} = 0 \quad \text{if } \lambda \geqslant 1, \tag{2.5c}$$

where G is shear modulus and $\boldsymbol{I}$ is unit tensor. This means that the passive stress in the muscle consists of an isotropic part $\boldsymbol{\sigma}_{\text{matrix}}$, following a Neo-Hookean material law (often used for rubbers) and a nonlinear part $\boldsymbol{\sigma}_{\text{fibre}}$ that only works in the fibre direction. In equation (2.5*c*) λ is the length change in the fibre direction. For the tendons and the passive behaviour of the muscle the same material law is used, but with different material parameters.

Within the context of the present paper, the active stress is more interesting to discuss. In the literature, Hill-type models are often chosen for the active stress. These are phenomenological models, accounting for the length–force and the velocity–force relationship of the muscle. In the present paper, a model based on the sliding-filament theory of Huxley (1957) is chosen, which was later adapted by Zahalak (1981). This also is a phenomenological model but at a different architectural level. A two-state Huxley model is used, which means that cross-bridges are either attached or detached. There are some disadvantages of this model, especially for rapid events, which have been extensively discussed in the literature (see Herzog 2000). However, for relatively slow phenomena the model gives good results, compared with experimental data (Maenhout *et al.* 2000).

The basic theory focuses on an ensemble of myosin heads, which are assumed to be capable of binding to actin, to form a cross-bridge. During contraction, a fraction of all cross-bridges is attached. Every attached cross-bridge has its own dimensionless attachment length ξ. The distribution of attached cross-bridges with respect to their length is given by the function $n(\xi,t)$ and the rate of change of this distribution can be expressed with a modified two-state Huxley equation:

$$\frac{\partial n(\xi,t)}{\partial t} - u(t)\frac{\partial n(\xi,t)}{\partial \xi} = r(t)f(\xi)[\alpha - n(\xi,t)] - g(\xi)n(\xi,t), \tag{2.6}$$

where $u(t)$ is the scaled shortening velocity of a half sarcomere, $f(\xi)$ and $g(\xi)$ are the attachment and detachment rate of the cross-bridges, respectively, α is an overlap factor, and $r(t)$ is an activation factor, depending on the amount of calcium in the myofibrillar space. It should be noted at this point that equation (2.6) again is a partial differential equation with a time derivative and a derivative to the attachment length, which is a microstructural property. The shortening velocity $u(t)$ is a macroscopic property.

The active muscle stress can be determined from the distribution of attached cross-bridges n. It is assumed that the cross-bridge force depends linearly on the attachment length ξ. The active Cauchy stress $\boldsymbol{\sigma}_{\text{a}}$ generated by all cross-bridges in a slice of half sarcomeres is described as

$$\boldsymbol{\sigma}_{\text{a}}(t) = c_{\text{a}}\lambda\int_{-\infty}^{\infty}\xi n(\xi,t)\,\mathrm{d}\xi = c_{\text{a}}\lambda Q_1(t), \tag{2.7}$$

where Q_1 is the first moment of function $n(\xi,t)$.

As can be seen from equation (2.7), the active stress σ_{a} does not depend on the exact shape but on the first moment of the function n, c_{a} is a material constant and represents the maximal isometric stress with the maximum number of cross-bridges attached and λ is the extension ratio in fibre direction. Zahalak (1981) has made plausible

that it is not always necessary to determine the exact distribution function n, but it suffices to determine the first moment Q_1. This will be used later to simplify the numerical procedure. (Also see equation (3.4).)

The functions $f(\xi)$ and $g(\xi)$ represent the rate for attachment and detachment, respectively, of myosin to actin. These functions have to be determined in experiments and depend on the type of species and the muscle type (fast twitch or slow twitch). The overlap factor α is a function of the actual length of a sarcomere and accounts for the region of the filaments that overlap and hence the number of cross-bridges that can be formed potentially. The activation factor $r(t)$ describes the calcium activation in the Huxley cross-bridge model and is used to trigger the muscle to contract or release the contraction.

It can be seen that if $r = 0$, the attachment term is zero and only the detachment term is active, such that the active stress will decrease. When $r > 0$ the attachment term plays a part in the equations and depending on the other factors on the right-hand side the number of attached cross-bridges (and thus the active stress) may either increase or decrease.

A myosin head can only interact with an actin binding site if two calcium ions are bound to the specific receptor sites on the troponin molecule of that actin site. The fraction activated actin is defined as $r(t)$:

$$r(t) = \frac{c^2}{c^2 + \mu c + \mu^2}, \tag{2.8}$$

with c representing the ratio of the free calcium concentration in the myofibrillar space with respect to the maximum myofibrillar calcium concentration and μ the troponin–calcium reaction ratio constant. The calcium concentration is regulated by the electric stimulation causing the release of calcium from the SR. Zahalak & Ma (1990), Ma (1988) and Zahalak & Motabarzadeh (1997) derived a model for the calcium activation dynamics, described by the following equations:

$$\frac{\mathrm{d}C_\mathrm{t}}{\mathrm{d}t} = \rho\left(1 - \frac{c}{c^*}\right)\chi(t) - \tau_0^{-1}\left(\frac{c}{c + k_\mathrm{m}}\right), \tag{2.9}$$

$$C_\mathrm{t} = c + 2bQ_0 + r\left(2 + \frac{\mu}{c}\right)(1 - bQ_0), \tag{2.10}$$

where C_t is the total calcium in the myofibrillar space. The first term on the right-hand side of equation (2.9) is the input rate of the calcium, with c^* the average calcium concentration in the muscle and ρ the increase in total calcium concentration due to one action potential. The stimulation function $\chi(t)$ is used to control the active stress in the muscle. The second term on the right-hand side of equation (2.9) represents the rate at which the calcium is pumped out of the cytoplasm into the SR and is based on the classic enzyme kinetics theory, with τ_0 and k_m as the Michaelis–Menten parameters. In equation (2.10) Q_0 is the zeroth moment of the actin–myosin bond distribution function $n(\xi,t)$ (see equation (3.4)).

To summarize, the equilibrium equations have to be solved in each point of the muscle. By prescribing the stimulation function $\chi(t)$, equation (2.9) allows a calculation of the total amount of free calcium $C_\mathrm{t}(t)$ in the cytoplasm and the amount of calcium $c(t)$ available for the cross-bridge attachment (equation (2.10)). With this information and equation (2.8) the activation factor $r(t)$ can be calculated and the Huxley equation (2.6) can be solved for time-step t. When the active stress is known at each point in the muscle the equilibrium equations, together with constitutive equations for the passive behaviour of muscle and tendon, can be solved and strains and total stress in the muscle calculated. There exists a coupling between the deformation of the muscle and the generated active stress by means of the contraction velocity $u(t)$ and the overlap factor α in equation (2.6). The finite element method is used to solve the partial differential (2.1). The reason for this is that the finite element method is the best suitable method to deal with complex geometries.

3. SOLUTION METHOD

The objective of the finite element method is to find approximate solutions for boundary value problems, governed by partial differential equations. Clearly the set of equations given in § 2 cannot be solved analytically. In the set of equations above, the unknowns are the displacements of material points in the muscle tissue as a function of position and time t, the hydrodynamic pressure P, the total calcium C_t and the free calcium c in the myofibrillar space.

The finite element method proceeds along three well-defined steps.

(i) Transformation of the original differential equation into an integral equation by means of the principle of weighted residuals.
(ii) Discretization of the solution by interpolation. If an approximate solution is found in a finite number of points (nodes) an approximation field may be constructed by interpolation between these points.
(iii) Using the discretization, the integral equation is transformed into a set of equations from which the nodal values of the unknowns can be solved.

First of all the differential equation is transformed into an integral equation by means of the weighted residual method. This procedure is applied to the equilibrium equation (2.1) and the incompressibility constraint, equation (2.2). For this the equations are written in a weak form (which will be explained below), by multiplying the momentum equation by an arbitrary weighting function $\boldsymbol{v}$ and the incompressibility condition by a weighting function q giving, after partial integration:

$$\int_\Omega (\nabla \boldsymbol{v})^\mathrm{T} : (-p\boldsymbol{I} + \tau)\, \mathrm{d}\Omega = \int_\Omega \boldsymbol{v}\cdot\boldsymbol{f}\, \mathrm{d}\Omega, \tag{3.1}$$

$$\int_\Omega q(\mathcal{J} - 1)\, \mathrm{d}\Omega = 0, \tag{3.2}$$

with $\mathcal{J} = \det\boldsymbol{F}$.

In equation (3.1) τ represents the total extra stress in the muscle, i.e. without the hydrostatic pressure and $\boldsymbol{f}$ in the right-hand side of equation (3.1) represents the external load. In these equations Ω represents the total volume

that is occupied by the modelled structures, i.e. the muscle and some tendons and connective tissue. It can be shown that the integral equations (3.1) and (3.2) are equivalent to the original partial differential equations, provided that the weighting functions can be chosen arbitrarily. Effectively, the method of weighted residuals transforms the requirement that a function must be equal to zero on a given domain at an infinite number of points, into a single number, the integral that must be equal to zero.

After partial integration second-order derivatives of the unknown displacement fields have disappeared from the equations and only first-order derivatives are found; therefore the differentiability requirements imposed on the solution are reduced. That is why equations (3.1) and (3.2) are called the weak form.

One of the problems with equations (3.1) and (3.2) is that the domain Ω changes as a function of the solution. The total volume does not change, but the shape does. Because the shape is unknown beforehand, the integral in the equation cannot be solved. That is why a reference configuration has to be chosen and the equations are rewritten with respect to this configuration. There are several ways do this, but in the present formulation an updated Lagrange procedure is chosen, meaning that the last converged state in the solution process is the reference configuration.

This leads to a nonlinear set of equations, with respect to the displacements and the pressures. This set can be linearized by means of a Newton–Raphson iteration process, which is the same as writing the left-hand side of equations (3.1) and (3.2) in a Taylor series around an estimated solution and ignoring higher-order terms in the series.

By dividing the domain into simple shaped sub-domains (elements), e.g. into triangles or quadrilaterals, spatial discretization within these sub-domains is straightforward. Furthermore, evaluation of the integral expression by means of numerical integration on these sub-domains is feasible.

To approximate the solution in each point of the domain it is necessary to use an interpolation scheme. In this case a different interpolation is chosen for the pressure compared with the displacements. The displacement field is quadratic and the pressure field is linear in the element. The element is from the Taylor–Hood family with a continuous interpolation field for the pressure. It satisfies the so called Babuska–Brezzi condition (Zienkiewicz & Taylor 1989) meaning that oscillations in the pressure field, due to the incompressibility, are avoided. Finally this leads to a set of algebraic equations that can be solved with standard methods:

$$\begin{bmatrix} \underline{M} & \underline{K}_{\mathrm{up}} \\ \underline{K}_{\mathrm{pu}} & \underline{0} \end{bmatrix} \begin{bmatrix} \delta\underline{s} \\ \delta\underline{p} \end{bmatrix} = \begin{bmatrix} \underline{f} \\ \underline{g} \end{bmatrix}, \tag{3.3}$$

where $\delta\underline{s}$ are the unknown incremental displacements in the nodes and $\delta\underline{p}$ are the unknown nodal pressures. The matrices on the left-hand side are integrals over the domain of the last converged incremental solution.

When the passive behaviour of the muscle is modelled as a visco–elastic material, or when active behaviour is involved, equation (3.3) becomes a time-dependent equation. In the present implementation each load step represents a time-step.

The active load is derived by prescribing a stimulation frequency as a function of time. By solving the algebraic equation (2.10) and integrating the ordinary differential equation (2.9) using a Euler explicit scheme the intermyofibrillar free calcium $c(t_i)$ as a function of time-step t_i is determined. This leads to a value of the activation function $r(t_i)$ at each time-step t_i. With a known $r(t)$ it is possible to solve the Huxley equation.

This is a partial differential equation that has to be solved in each integration point of the finite element mesh. In principle this is possible; however, $n(\xi,t)$ has to be stored at a large number of discrete values of the attachment length ξ in each integration point and at each time-step. This requires a lot of computer memory and data transport. Although it is possible with modern computers it is not the most efficient way.

It is possible to transform the partial differential Huxley equation into an approximate set of three ordinary differential equations by means of the DM method as derived by Zahalak (1981).

In general the kth moment of a distribution function n is defined as

$$Q_k(t) = \int_{-\infty}^{\infty} \xi^k n(\xi,t)\, \mathrm{d}\xi. \tag{3.4}$$

As can be seen from equation (2.7), the active stress σ_a does not depend on the exact shape but on the first moment of the function n.

It is possible to transform the partial differential Huxley equation into an infinite set of coupled linear ordinary differential equations, which is equivalent to the original Huxley equation. By postulating *a priori* a reasonable shape for the function n, a closed set of differential equations can be determined, meaning that the number of equations is equal to the number of unknowns. By assuming a normal distribution for the function n, Zahalak approximated the partial differential Huxley equation (2.6) by the following set of ordinary first-order differential equations:

$$\mathrm{d}Q_0/\mathrm{d}t = b_0 - f_0(Q_0,Q_1,Q_2), \tag{3.5a}$$

$$\mathrm{d}Q_1/\mathrm{d}t = b_1 - f_1(Q_0,Q_1,Q_2) - u\,Q_0, \tag{3.5b}$$

$$\mathrm{d}Q_2/\mathrm{d}t = b_2 - f_2(Q_0,Q_1,Q_2) - 2u\,Q_1. \tag{3.5c}$$

The functions f_0, f_1 and f_2 have been defined in Zahalak (1981).

Now in each point in time and at each integration point, with known $r(t_i)$, $\lambda(t_i)$ and $u(t_i)$ and the moments $Q_\lambda(t_i)$ it is possible to calculate the moments $Q_\lambda(t_{i+1})$ by either a Euler explicit scheme or a two- or four-step Runge–Kutta time integration. The active stress is derived from the first moment by means of equation (2.7).

To illustrate the potential of this model for skeletal muscle, it is applied to describe the mechanical behaviour of the TA muscle of a rat.

4. A MODEL OF A TIBIALIS ANTERIOR OF A RAT

The muscle geometry was derived from normal high-resolution MRIs (figure 1*a*). The fibre directions were

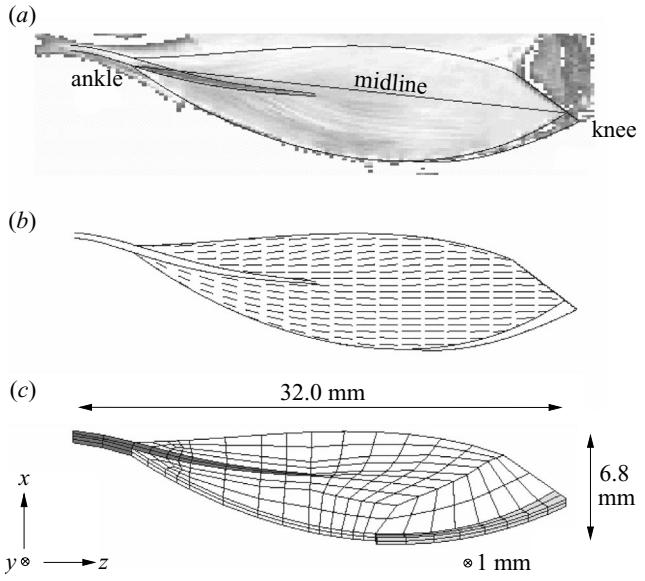

Figure 1. A 2D continuum model of the cross-section of the mid-sagittal plane of the TA of the rat. (*a*) Geometry of the model derived from MRI, (*b*) fibre direction, and (*c*) finite element modelling grid. The distal tendon is dark grey and the proximal aponeurosis is light grey.

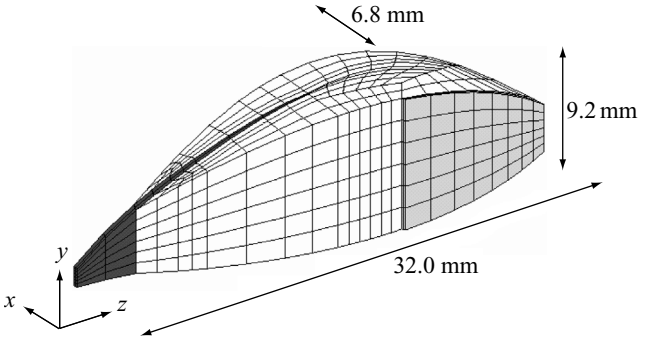

Figure 2. A 3D model of the TA.

measured with diffusion tensor imaging and were described by polynomial fits of the measured directions (Van Donkelaar *et al.* 1999; Van Doorn *et al.* 1996). This resulted in a geometry and fibre direction as shown in figure 1*b*. The geometry was divided into iso-parametric quadratic elements as shown in figure 1*c*. For the 3D model, three elements were used in the transverse direction. The surface of the model representing the medial side was chosen to be flat, while the surface representing the lateral side was given a curvature as shown in figure 2. The fibre directions in the transverse direction are chosen parallel to the curvature in this direction.

To interpret the simulation results and compare them with the MRI studies, the midline of the model is defined in a way similar to the MRI experiments. The orientation of the midline is shown in figure 3. For the 3D model the midline cuts through the TA geometry at $y = 3$ mm based on the definition of the midline in the SOO as defined in Maenhout (2002).

The material parameters for the contraction model were partly obtained from independent experiments described in the literature and partly estimated on the basis of torque measurements on stimulated muscles. The model parameters for the DM model are given in table 1.

The model parameters for the calcium activation model were determined by Zahalak & Ma (1990) and are given in table 2. The parameters for the passive behaviour of the muscle were determined by fitting the muscle model on MRI data. The boundary conditions were also determined by means of MRI experiments.

Figure 4 gives an example of a typical result. The local strains during tetanic contraction of the TA are given. The total force generated by the muscle in this simulation 9.8 N (Maenhout *et al.* (2000) measured 14.6 ± 3.4 N). The muscle tendon complex is kept at a fixed length. The strain E_{xx} is the normal strain in the z-direction, along the length axis of the muscle (note, that this is not identical to the muscle fibre direction). E_{xx} and E_{yy} are the normal strains in the x and y direction, respectively, both perpendicular to the length direction of the muscle. The sagittal and transverse strains are positive (*ca.* 0.03) in the mid-area of the TA, meaning that the muscle becomes thicker during contraction. The longitudinal strains are negative (*ca.* -0.05), implying of course that the muscle shortens. At the muscle ends the opposite is valid; sagittal and transverse strains are negative, while the longitudinal strains are positive. The latter is due to the fact that the whole muscle tendon complex is held at the same length (isometric contraction). The fairly stiff tendon and fascia and the passive muscle properties result in a rather complex stress–strain state in this part of the muscle. When properties of the tendon or the passive muscle complex change, for example due to surgical intervention or disease, the local stress–strain state may change and the muscle will start to adapt. The present model enables us to study these changes at a local level.

Figure 5 shows strains at the surface of the muscle in the simulations. These are compared with experimentally determined strains of isometric contractions of rat TA. Superficial local fibre strains were measured by 3D-video analysis of surface markers (Maenhout 2002). Figure 5 shows that surface strains are positive at the muscle ends and negative in the middle of the muscle. This is found in the simulations and in the experiments. It is also clear that, although qualitatively the same trend is seen, there are considerable quantitative differences. The experimental strains are higher than those obtained numerically. Moreover, the minimum lies at a different position. The latter is important, because the primary objective of the model was to determine this inhomogeneous strain distribution.

5. DISCUSSION

The objective of the present paper was to explain the basic concepts of the finite element method and to show its abilities on a model of a biological structure. For this, a recently developed continuum model for contracting skeletal muscle was chosen, because it illustrates nicely that one of the major complexities in this type of analysis is caused by the difficult constitutive behaviour of the material. This especially is true for muscle, because apart from the nonlinear passive properties, it has an active component. Muscle is able to generate force by itself. It is this active stress and the coupling of this stress with the

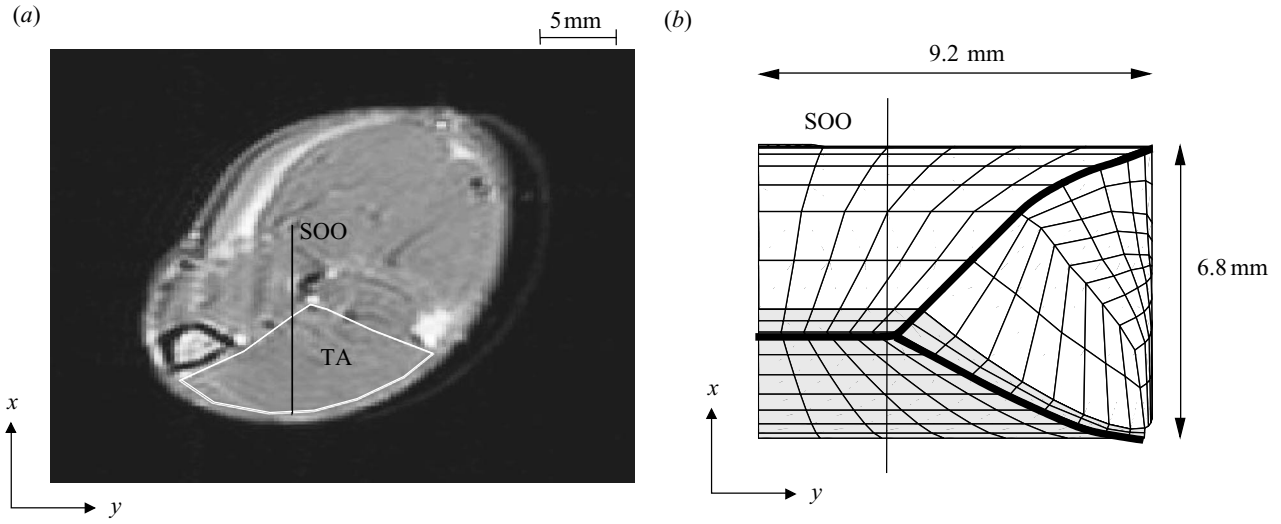

Figure 3. Representation of the TA in the transverse (x–y) plane. (*a*) Spin echo image of the central transverse slice with the definition of the SOO. The x-direction conincides with the sagittal (superficial–deep) direction and the y-direction coincides with the transverse (medial–lateral) direction. (*b*) 3D model of the TA as already shown in figure 2 with the viewpoint in the proximal–distal (z) direction.

Table 1. Parameter values of the DM model.

parameter	f_1	g_1	g_2	g_3	μ
value	163[a]	64[a]	200[b]	30[b]	0.2[c]
dimension	s^{-1}	s^{-1}	—	—	—

[a] Maenhout *et al.* (2000).
[b] Zahalak (1981).
[c] Hatze (1981).

Table 2. Parameters that were used in the model for the calcium activation.

parameter	ρ	τ_0	k_m	B	τ
value	2.9	9.2	0.006	0.77	2.9
dimension	—	ms	—	—	ms

deformation and deformation rate that makes this type of analysis complicated.

Keeping in mind that determining the inhomogeneous strain distribution in the muscle was the objective of the modelling, it is clear that the authors have not reached their goal yet. Qualitatively, the result is in agreement with experiments, but quantitatively the difference between calculated and measured strains is too large. There is one obvious improvement that still has to be implemented which may have a large influence on the results. Although the geometry of the mid-sagittal plane of the muscle is described reasonably well, in the transverse plane the geometry deviates a lot from the real muscle (compare figure 3*a*,*b*). It is clear from, for example, heart models (Bovendeerd *et al.* 1994) that the geometry, and especially the local fibre direction, has a large influence on the results. It may very well be that improving the geometry (for which the data are already available from MRI measurements) will result in higher strains with a hopefully more realistic distribution.

This type of model is complex, with many material parameters and difficult to validate. One might wonder if this complexity is necessary and if it would not be possible to reach the same or even better results with much simpler representations of the real muscle. Many examples can be found in the literature, where sometimes extremely simple abstractions of reality resulted in a better understanding of otherwise very complex phenomena. Also for contracting muscle, much simpler models have been used in the past, which were fairly successful. Many gait analysis problems can be solved by using 1D-line elements for muscle with simple contraction models.

However, sometimes the level of complexity as invoked in the present paper is unavoidable. Research on technical materials in the last two decades has shown that to understand phenomena related to damage, adaptation or ageing, it is necessary to incorporate the microstructure of these materials in the analysis. This has even led to multi-level finite element models in which different length scales are integrated into one single analysis (Smit *et al.* 1998; Kouznetsova *et al.* 2001). It has been shown that this method can be used to predict macroscopic material behaviour by looking at the microscale and to use that as a tool to design new improved materials. Recently this method has also been proposed for biological materials (Breuls *et al.* 2002).

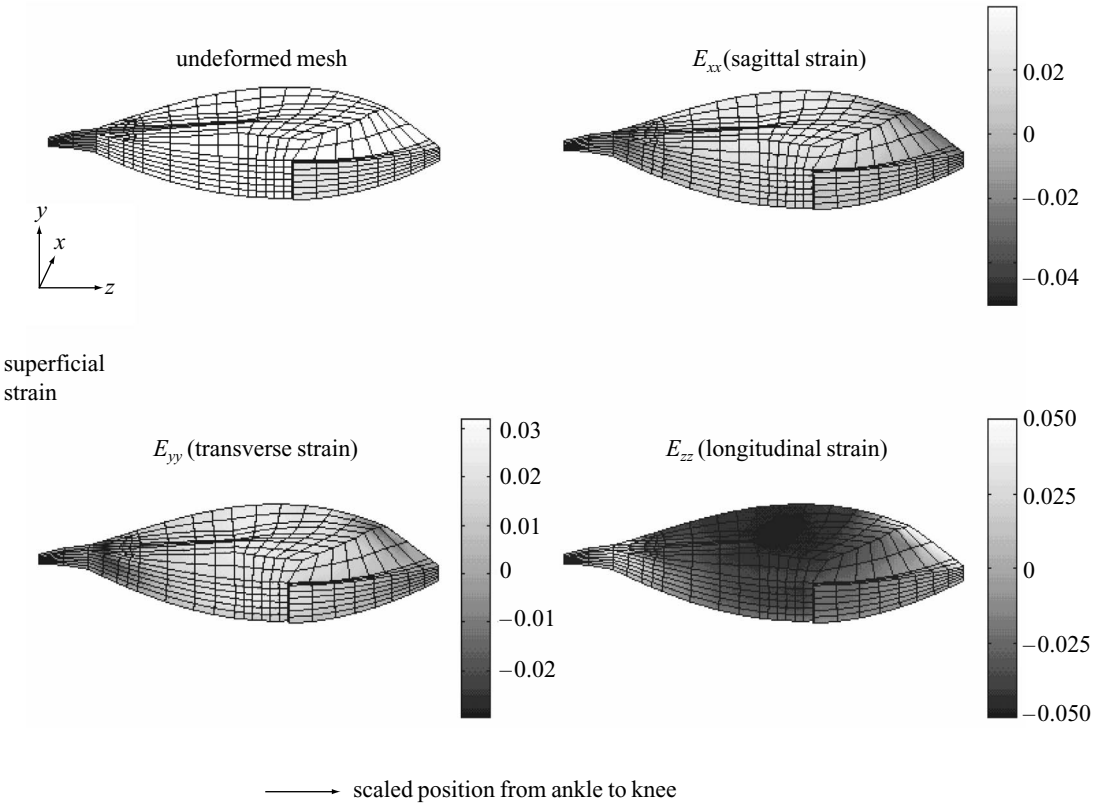

Figure 4. Simulated strain field of the TA. The strain components according to the global x,y,z-coordinate system are given at the time that the muscle is in tetanic contraction.

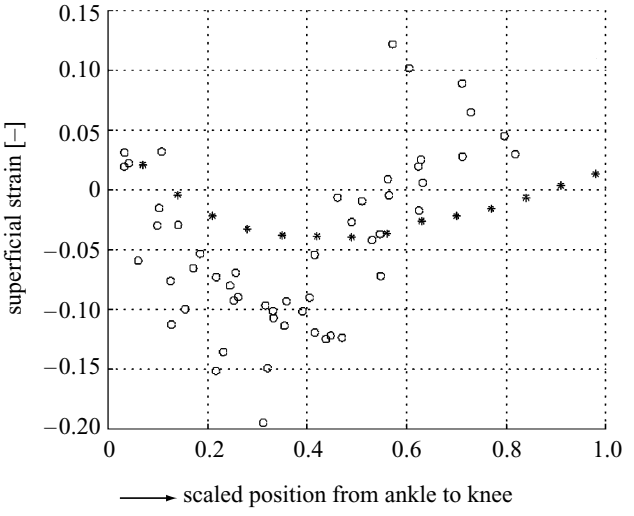

Figure 5. Measured (video (open cicles), seven rats) and simulated (asterisks) Green Lagrange strains at the surface of the TA in a line from distal to proximal.

The same is true for skeletal muscle. If we want to understand how muscle adapts to changes in the mechanical state, we have to know local stresses and strains and this can only be done by means of models that spawn such results. Regarding the number of fibres present in a skeletal muscle, the only feasible way to do this at present is to use an anisotropic continuum model like the one used in this paper. However, it is not unlikely that in the near future a multi-level approach has to be applied to account for the typical micro-structure of the muscle.

6. NOTATION AND NOMENCLATURE

a	scalar
$\boldsymbol{a}$	vector
$\underline{a}$	column with scalars
$\boldsymbol{A}$	second-order tensor
A	matrix
$\boldsymbol{A}\cdot\boldsymbol{a}$	inner product of second-order tensor with vector
tr$\boldsymbol{A}$	trace of a tensor
:	double dot product $\boldsymbol{A}:\boldsymbol{B}=\mathrm{tr}(\boldsymbol{A}\cdot\boldsymbol{B})$
det$\boldsymbol{A}$	determinant of second-order tensor $\boldsymbol{A}$
$\boldsymbol{\sigma}$	Cauchy stress tensor
$\boldsymbol{F}$	deformation tensor
$\boldsymbol{I}$	unit tensor
G	shear modulus
P	hydrodynamic pressure
λ	extension ratio
$n(\xi,t)$	distribution of attached cross bridges with attachment length ξ
$u(t)$	scaled shortening velocity of a half sarcomere
$f(\xi)$, $g(\xi)$	attachment and detachment rate, respectively
$r(t)$	Calcium activation factor (between 0 and 1)
α	overlap factor
Q_i	ith moment of the function $n(\xi,t)$
C_{t}	total amount of calcium in the cytoplasma
c	ratio of the free calcium concentration with respect to the maximum calcium concentration in the cytoplasma
$\delta\underline{s}$	unknown incremental displacements in the nodes
$\delta\underline{p}$	unknown incremental pressures in the nodes

REFERENCES

Bovendeerd, P. H., Huyghe, J. M., Arts, T., Van Campen, D. H. & Reneman, R. S. 1994 Influence of endocardial–epicardial crossover of muscle fibres in left ventricular wall mechanics. *J. Biomech.* **27**, 941–951.

Breuls, R. G., Sengers, B. G., Oomens, C. W., Bouten, C. V. & Baaijens, F. P. 2002 Predicting local cell deformations in engineered tissue constructs: a multilevel finite element approach. *J. Biomech. Engng* **124**, 198–207.

Gielen, A. W. J., Oomens, C. W. J., Bovendeerd, P. H. M., Arts, T. & Janssen, J. D. 2000 A finite element approach for skeletal muscle using a distributed moments model of contraction. *Comp. Meth. Biomech. Biomed. Engng* **3**, 231–244.

Hatze, H. 1981 *Myocybernetic control models of skeletal muscle: characteristics and applications*. Mucklneuk, Pretoria: University of South Africa.

Herzog, W. (ed.) 2000 *Skeletal muscle mechanics: from mechanisms to function*. Chichester: Wiley.

Hunter, S. C. 1983 *Mechanics of continuous media*, 2nd edn. Chichester: Wiley.

Huxley, A. F. 1957 Muscle structure and theories of contraction. *Prog. Biophys. Biophys. Chem.* **173**, 257–318.

Kouznetsova, V., Brekelmans, W. A. & Baaijens, F. P. 2001 Approach to micro-macro modeling of heterogeneous materials. *Comput. Mechan.* **27**, 37–48.

Ma, S. P. 1988 Activation dynamics for a distributed moment model of muscle. PhD thesis, Washington University, St Louis, MO, USA.

Maenhout, M. 2002 Strain fields within contracting muscle. PhD thesis, Maastricht University, The Netherlands.

Maenhout, M., Hesselink, M. K. C., Oomens, C. W. J. & Drost, M. R. 2000 Parameter identification of a distributed moment approximated two state Huxley model of the rat tibialis anterior muscle. In *Skeletal muscle mechanics* (ed. W. Herzog), pp. 135–154. Chichester: Wiley.

Smit, R. J., Brekelmans, W. A. & Meijer, H. E. 1998 Prediction of the mechanical behavior of nonlinear heterogeneous materials by multi-level finite element modeling. *Comp. Meth. Appl. Mech. Engng* **155**, 181–192.

Van Donkelaar, C. C., Kretzers, L. J. G., Bovendeerd, P. H. M., Lataster, L. M. A., Nicolay, K., Janssen, J. D. & Drost, M. R. 1999 Diffusion tensor imaging in biomechanical studies of skeletal muscle function. *J. Anat.* **194**, 79–88.

Van Doorn, A., Bovendeerd, P. H. M., Nicolay, K., Drost, M. R. & Janssen, J. D. 1996 Determination of muscle fibre orientation using diffusion-weighted MRI. *Eur. J. Morphol.* **34**, 5–10.

Zahalak, G. I. 1981 A distributed moment approximation for kinetic theories of muscular contraction. *Math. Biosci.* **55**, 89–114.

Zahalak, G. I. & Ma, S. P. 1990 Muscle activation and contraction: constitutive relations based on cross-bridge kinetics. *J. Biomech. Engng* **112**, 52–62.

Zahalak, G. I. & Motabarzadeh, I. 1997 A re-examination of calcium activation in the Huxley cross-bridge model. *J. Biomech. Engng* **119**, 20–29.

Zienkiewicz, O. C. & Taylor, R. L. 1989 *The finite element method*, 4th edn. New York: McGraw-Hill.

GLOSSARY

DM: distributed moments
MRI: magnetic resonance imaging
SOO: slice of observation
SR: sarcoplasmatic reticulum
TA: tibialis anterior